Effect of Barrier Walls on Detection of Breathing Vital Signs with Through-Wall Radar

Fildha Ridhia[1], Aloysius Adya Pramudita[2], Yuyu Wahyu[3], Harfan Hian Ryanu[4]

***Abstract*—Through-Wall Radar (TWR) has been extensively applied in various fields, one of which is in the search for, or evacuation of disaster victims struck by rubbles. The TWR is an application of radar systems operating in a wide frequency range or ultra-wideband (UWB), hence it has a high accuracy level in detecting objects behind walls. In this study, the Vivaldi antenna was used to obtain a high-level resolution for its capability to operate on UWB. Parameters such as dielectric characteristics are needed for each barrier type to generate a high accuracy level. The experiment was conducted to determine the effect of barrier walls on the detection of vital signs of respiration using a radar system modeled using two methods, namely, a vector network analyzer (VNA) and bladeRF. The experiment stages included the making of the experimental system design, experimental data collection, experimental data processing, and experimental results analysis. Wall types used in this study were brick and wooden walls. The experimental data results were used to analyze the effect of the barrier on the detection of vital signs of respiration using a radar system. Experiments using VNA as a radar system were conducted to analyze the effect of the barrier wall on the detection of the target behind the barrier wall. Experiments using bladeRF as a radar system were conducted to prove the presence or absence of a barrier effect on the detection of vital signs of respiration using a radar system. The measurement results showed that the largest peak-to-peak signal amplitude decrease occurred in the target detection with a distance of 125 cm, which was 11.51 dB, and a delay of 0.084 ns when using the Hebel brick barrier. Meanwhile, in wooden barriers, the average decrease in peak-to-peak signal amplitude was 2.968 dB, and the delay was 0.006 ns.**

***Keywords*—Through-Wall Radar (TWR), Respiratory, Barrier, BladeRF.**

I. INTRODUCTION

Indonesia's tectonic conditions, dubbed as the Ring of Fire, make almost all regions of Indonesia prone to natural disasters, one of which is an earthquake that can lead to many fatalities. The lack of technology to accurately locate the victim's location makes the victim evacuation hindered, resulting in many victims are unable to be rescued alive. It has encouraged scientists to continue developing a technology that can detect the presence of humans behind walls by using radar systems.

A through-wall radar (TWR) is one of the radar applications emitting electromagnetic waves that can penetrate the wall and receive reflections from certain objects behind the wall [1]. TWR is used to generate good wall penetration by working on very wide bandwidths, thus having the potential to detect small displacements, such as chest wall movement in breathing [2]. The antenna used for the TWR system has several special requirements, including having a directional radiation pattern, high gain, and very wide bandwidth. One antenna that meets these requirements is the Vivaldi antenna [3].

In [4], a breathing detection radar experiment was conducted using a performance network analyzer (PNA) and a Doppler radar with horn-type antennas at a frequency of 10 GHz. In addition, in [5], the same experiment was conducted using SIMO radar at a center frequency of 800 MHz. Breathing detection radar using ultra-wideband impulse radar (UWB) has also been discussed in [6], [7]. Meanwhile, in [8], breathing detection experiments with UWB MIMO imaging radar were shown. From the study, results showed that radar could detect vital signs of breathing behind walls. However, previous studies did not specifically discuss the significance of the barrier effect on the detection of vital signs of breathing using radar systems.

In this study, experiments were conducted using a vector network analyzer (VNA) and bladeRF as modeling of the radar system. Measurement using VNA was intended to determine the effect caused by the barrier wall through the total attenuation and delay values. Measurements using VNA cannot detect breathing patterns in real time, so breathing pattern detection was done with bladeRF as a radar system. Measurements using bladeRF are aimed at identifying the effect of the barrier on the detection of vital signs of breathing behind walls.

II. METHODOLOGY

A. Ultra-Wideband (UWB)

UWB radar is a system that uses electromagnetic waves to detect and measure the distance of an object [9]. The radar operates by emitting an electromagnetic wave, which then hits an object, and receives back the reflected wave from the detected object. The reflected signal from the object provides information regarding the range or distance of the target. The target distance can be recognized from the time it takes for electromagnetic waves to hit the target and be again received by the radar [10]. Radar can detect small displacements in the body, such as detecting breathing through the movement of the chest wall when inhaling and exhaling. The radar requires a high resolution to detect small displacements, i.e., the radar system must have a wide bandwidth [2].

The basic principle of how UWB radar works is that it will initially generate a short signal in the form of an

[1,2,4] *Intelligent Sensing-IoT Center, Telkom University, Jl. Telekomunikasi No. 1, Terusan Buahbatu, Bandung 40257, Indonesia (email: [1]fildhar@student.telkomuniversity.ac.id, [2]pramuditaadya@telkomuniversity.ac.id, [4]harfanhr@telkomuniversity.ac.id)*

[3] *BRIN, Gedung B.J. Habibie, Jl. M.H. Thamrin No. 8, Jakarta Pusat 10340, Indonesia (email: [3]yuyu003@lipi.go.id)*

[Received: 4 April 2022, Revised: 3 August 2022]

electromagnetic wave and transmit it via the transmitting antenna. When the transmitted signal hits the object, it is reflected back by the object to the receiving antenna and received by the UWB radar. The delay between the sender and receiver signals is the distance between the Tx – object – Rx. UWB radar has several advantages, including being able to penetrate barriers, having good wall penetration, not requiring direct contact with objects, being low power, portable, and low cost [11], [12].

B. Through-Wall Radar (TWR) System

TWR is a radar application that emits electromagnetic waves that can penetrate walls and receive reflections from certain objects behind walls [1]. The TWR system is capable of detecting the distance and angle of the object being detected [2]. The TWR work system starts from the radar system consisting of processing block, transmitter (Tx), receiver (Rx), antenna, and display. In the processing, signals are processed and set before they are sent to Tx and after they received by Rx. The Tx functions as a processing before it is emitted by the antenna, while the RX functions as a signal processor after it is received by the antenna. The display serves as an interface so that the signal shape is visible to humans.

Subsequently, electromagnetic waves or signals emitted by the Tx antenna will hit the surface of the wall. Signals propagating through two mediums have two possibilities, i.e., reflected or forwarded. When an electromagnetic wave propagates through a medium, it has a propagation constant that can be written on (1).

$$\gamma = \alpha + j\beta \tag{1}$$

where α and β are damping constants and phase constants whose values depend on the type of medium propagated by the wave.

C. Wave Propagation Through-Walls

Waves propagating on a perfect dielectric medium have a value of $\alpha = 0$, so the value of the propagation constant is only a value of β. Meanwhile, waves propagating through the dielectric medium are imperfect and have α values, with α and β values being written on (2) and (3).

$$\alpha\,(real) = (2\pi f)\sqrt{\frac{\mu\varepsilon\prime}{2}}\left(\sqrt{1+\left(\frac{\varepsilon"}{\varepsilon\prime}\right)^2}-1\right)^{\frac{1}{2}} \tag{2}$$

$$\beta(imajiner) = (2\pi f)\sqrt{\frac{\mu\varepsilon\prime}{2}}\left(\sqrt{1+\left(\frac{\varepsilon"}{\varepsilon\prime}\right)^2}+1\right)^{\frac{1}{2}} \tag{3}$$

where f is the utilized frequency, μ is the wall permeability, ε' is the real permittivity of the medium, ε'' is the imaginary permittivity of the medium, and μ is the medium permeability.

The tests in this experiment used two different types of walls, i.e., Hebel brick walls, with dielectric constants $\varepsilon' = 2.85$ and $\varepsilon" = 0.285$, as well as wooden walls with dielectric constants $\varepsilon' = 1.99$ and $\varepsilon" = 0.159$ [13].

Due to the presence of a barrier wall in the detection, attenuation and delay will appear in the detection results. Signal attenuation is caused by the barrier and the distance travelled by the wave when propagating towards the object and back to the radar. Delay is the delay time caused by the presence of a barrier during detection, causing a shift in position at the peak of the reflected signal received by the radar. To determine the total attenuation (α_{Total}), delay (Δt), and position shift (ΔS) of signal peaks, calculations were made using (4) to (7), with ℓ being the barrier thickness.

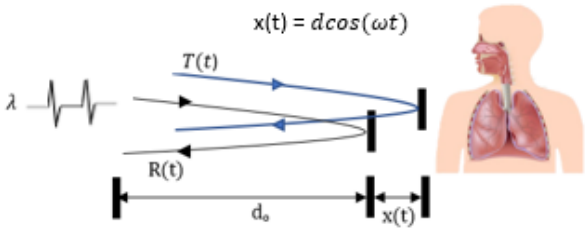

Fig. 1 Periodic movement of the chest wall.

$$\alpha_{Total}(\,dB) = 2 \times \ell \times \alpha \tag{4}$$

$$v = \frac{2\pi f}{\beta} \tag{5}$$

$$\Delta t = \frac{s}{v} \tag{6}$$

$$\Delta S = \frac{C \times \Delta t}{2} \tag{7}$$

where s being the radar distance from the barrier and C being the fast rate of light propagation, which is 3×10^8 m/s.

D. Chest Wall Movement in the Breathing System

The breathing system is one of the vital signs in humans. Human breathing is generally a periodic movement that can be seen from the movement of the chest wall or stomach. When inhaling air, the chest wall will dilate. It is because air enters the lungs so the lung volume increases. At the time of exhalation, the lung wall contracted because the lung volume is reduced, so that the air comes out [14]. The relationship between breathing and chest wall movement can be illustrated in Fig. 1, where $T(t)$ being the wave transmitted from the sending antenna, $R(t)$ being the signal reflected by the object, and $d_o + x(t)$ is the distance of the human being from the radar. This small movement in breathing activity is one of the characteristics that can distinguish humans from dead objects when detected using a radar system. The movement of the chest wall and wave propagation are made in the time domain, so that the changes can be analyzed by looking at the amplitude when inhaling and exhaling air.

E. Vivaldi Antenna

Antenna is a device that functions to transmit and receive electromagnetic waves. In applying a TWR system, an antenna with a compact and lightweight design is needed to be easily moved [15]. Antennas for TWR systems have several special requirements: directional radiation patterns, high gain, and very wide bandwidth. One antenna that meets these requirements is the Vivaldi antenna [3]. Gipson first created the Vivaldi

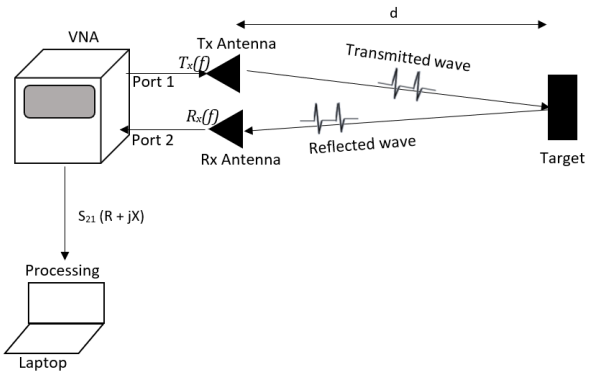

Fig. 2 Radar system modeling on VNA.

antenna in 1979 [16]. Based on [2], the Vivaldi antenna is a special antenna of tapered slot antenna (TSA) in exponential form or commonly known as an exponentially tapered slot antenna (ETSA). The narrow bandwidth on microstrip antennas can be overcome by using Vivaldi microstrip antennas with a wide bandwidth [17]. The main mechanism of the Vivaldi antenna is electromagnetic waves that propagate at the end of the exponential curvature of the Vivaldi arms so that the antenna can operate in a wide frequency range [17].

F. Radar System Modelling on Vector Network Analyzer (VNA)

VNA is a measuring instrument used to measure scattering parameters, namely S_{11}, S_{21}, S_{12}, and S_{22} of a system [18]. The parameters measured by the VNA are far-field and near-field parameters on the antenna. VNA has many settings that can be adjusted to the needs of the experiment.

The VNA radar system modeling has two ports considered as transmitters and receivers. Port 1 on the VNA functions as a transmitter (Tx) and port 2 as a receiver (Rx). The measurement result of S_{21} shows a transfer function describing the relationship between the transmitted and the received signals. The data taken in the S_{21} measurement uses a complex format mode (R + jX), resulting in a complex number consisting of real and imaginary components. S_{21} represents the power transferred from port 1 to port 2 expressed in the transfer function in (8).

$$H(f) = \frac{R_x(f)}{T_x(f)} = S_{21}. \quad (8)$$

The signal reflected by the object and received by the antenna Rx may be determined in (9)

$$R_x(f) = S_{21}T_x(f) \quad (9)$$

where $T_x(f)$ is the spectrum of the signal emitted by the radar system. To reconstruct the shape of the receive signal in the time region, Fourier transform inverse calculation [2] was performed as in (10).

$$R_x(t) = F^{-1}[R_x(f)]. \quad (10)$$

Signals reconstructed into the time domain were filtered in the form of signals with monocycle pulse shapes to clarify the reflections of the signals received by the antenna to be easier to analyze.

(a)

(b)

Fig. 3 Experimental scenario design using VNA, (a) using Hebel barriers, (b) using wooden barriers.

G. Software-Defined Radio (SDR)

Software-defined radio (SDR) is a technology in wireless communication that can be configured or reprogrammed using software [19]. Most of the processing in SDR occurs in hardware, and wave generation and the conversion are done in software [20]. The use of SDR can be more flexible because they can be configured or reprogrammed without having to replace the hardware [19]. In addition to their flexible nature, SDR can also minimize expenditures on radar system components due to their advantages, which include their ease of configuration, simplicity, and ability to reduce size [19].

H. GNU Radio

GNU Radio is a software that provides signal processing techniques to implement an SDR. GNU Radio uses an inexpensive radio frequency hardware or the simulation results [21]. GNU Radio users can design, simulate, and broadcast radio communication systems. Most radio communications that can use GNU Radio software are audio processing, mobile communications, satellite tracking, radar systems, as well as GSM and CDMA networks. GNU Radio is capable of working if it has an external radio frequency (RF) device. Application programs on GNU Radio generally use the Python programming language, but during implementation it can also be combined with the C+ + programming language for more accurate results [22].

I. BladeRF

The bladeRF is an SDR designed for users to explore wireless communication. It is a hardware incorporated with GNU Radio as a radar system model. In addition, baldeRF can

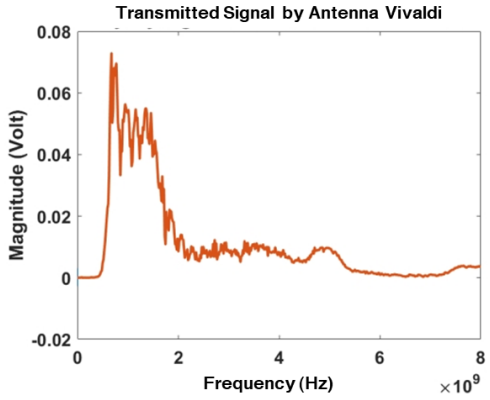

Fig. 4 Transmitted signals of the Vivaldi antenna.

be connected with a MATLAB-installed laptop to transmit or receive tests [23].

III. System Model

The system design in this study is generally shown in Fig. 2. The radar system was modeled using VNA, and GNU Radio with bladeRF. The object of this experiment was a metal plate and the movement of the chest wall in humans while breathing. Two types of barrier walls were used to determine the effect of barrier walls on breathing detection, namely Hebel brick and wooden walls.

A. Radar System Design with VNA

The overall design of the radar system using VNA is shown in Fig. 3. The VNA functions as a radar system and emits signals through the Vivaldi antenna. The signal evoked by the VNA has a frequency range of 300 kHz – 8 GHz with a center frequency of 4 GHz. Fig. 4 shows the signal transmitted by the antenna that has been affected by return loss. The most dominant signal was in the frequency range of 1 – 2 GHz. In this study, the employed S parameter was S_{21}, representing the power transferred from port 1 to port 2. Data was stored in VNA with a (R + jX) complex mode of 501 points. The evoked radar signal was in the form of monocycle pulses with a pulse width of 0.5 ns. The MATLAB R2018a software was used in the processing section to reconstruct the signal. Then, the results were displayed through a display in the form of a laptop. In accordance with Fig. 4, the test using VNA was carried out under two different conditions, i.e., with and without using Hebel brick and wooden barriers.

B. Radar System Design Using BladeRF

The radar system was modeled on GNU Radio as well as bladeRF with two ports for transmitters and receivers. The specifications for the radar in bladeRF were modeled in the GNU Radio software with an operating frequency of 2 GHz. The antenna served as a signal transmitter and receiver of signals reflected by the object. The signals received by the antenna were processed on GNU Radio. MATLAB was used to map data on graphs. Then, the results of signal processing were displayed through the display. Commensurate with Fig. 5, the test using GNU Radio and bladeRF was carried out under two

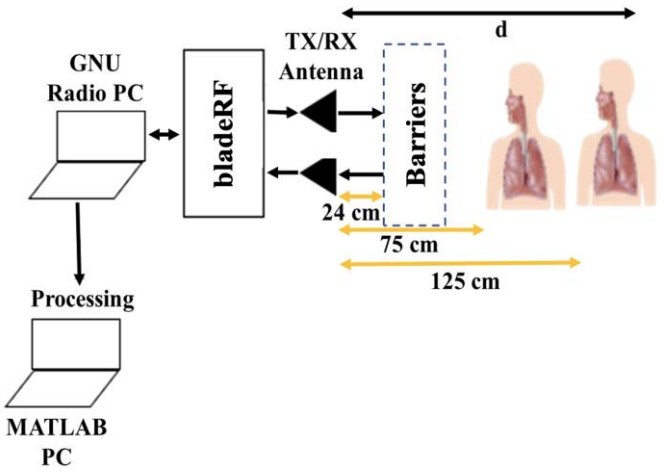

Fig. 5 Experimental scenario design using bladeRF with and without wall barrier.

different conditions, i.e., with and without using Hebel brick and wooden barriers in the operating frequency of 2 GHz.

C. Data Processing

Data processing in this experiment was carried out using a laptop/PC with MATLAB R2018a software. Based on [18], data processing on measurement results using VNA was carried out in six stages, as follows.

1. Compiling S_{21} data on MATLAB into fast Fourier transform (FFT) vectors in the frequency domain.
2. Performing the process of evoking a Tx transmit signal then converted into a discrete vector $T_x(n)$, with n as many as the number of S_{21} data, which was 501.
3. Calculating FFT from $T_x(n)$.
4. Performing a convolution using (11) with k = 1.

$$[R_x(k)] = \text{FFT}\,[S_{21}]\,.\,\text{FFT}[T_x(n)] \quad (11)$$

5. Determining signal received using inverse fast Fourier transform (IFFT), as seen in (12).

$$[R_x(n)] = \text{IFFT}\,[R_x(k)] \quad (12)$$

6. Signals reconstructed into the time domain were filtered in the form of signals in the monocycle pulse form to clarify the signal reflections received by the antenna to be easier to analyze.

Data processing on the test results using bladeRF was already in the time domain and could differentiate chest wall movements when inhaling and exhaling air. Hence, data processing on MATLAB was useful for mapping data on the chart to be analyzed.

Experimental data using VNA were analyzed to determine the presence of barrier effects. The barrier effect was sought by measuring the magnitude of loss occurring when the wave propagation traveled through the barrier wall compared to wave propagation without traveling through the barrier. Meanwhile, the data from the experimental results using bladeRF were analyzed to validate the effect of the barrier wall on the detection of chest wall movement when inhaling and exhaling air behind the wall.

TABLE I
MEASUREMENT RESULTS USING CALCULATIONS

Calculations	Hebel Brick Wall	Wood
α (Nepper/m)	7.06	4.7
β (rad/m)	141.61	118.27
Total attenuation (dB)	12.1	1.63
Delay (ns)	0.563	0.094

IV. RESULTS AND DISCUSSION

A. Measurement Results Using Calculations

Measurement results using the calculations in (2) to (7) show that each barrier provides losses with a certain value whose magnitude is affected by the dielectric constant value. Values of the losses could be determined by calculating the values of α and β. The α value was used to determine the total attenuation occurring when waves propagate through the barrier wall. Table I shows that the total attenuation produced by the Hebel brick barrier is 12.1 dB with a 10 cm-thick Hebel brick, while the total attenuation produced by the wooden barrier is 1.63 dB with a 2 cm-thick wood.

The value of β was used to calculate the delay experienced by waves as they propagated through the barrier wall. Delay affected the wave's travel time to the object and to reflect back towards the radar, so the value of β affected the shift of the signal's peak position when the radar detected it. Measurement results using calculations revealed that each barrier caused a delay with a certain value, the amount of which was affected by the dielectric constant value of the barrier used. In accordance with Table I, the delay produced by the Hebel brick barrier was 0.563 ns with a 10 cm-thick Hebel brick, while the delay produced by the 2 cm-thick wood barrier was 0.094 ns. From these calculations, it can be concluded that Hebel bricks provide greater attenuation and delay than wood.

B. Measurement Results Using VNA

The data were retrieved with complex mode ($R+jX$). The purpose of observing the S_{21} value was to find out the losses seen from the decrease in power and delay caused by the barrier when the wave propagated. The total attenuation was obtained from the difference of peak-to-peak amplitude between the signal with and without using a barrier written in (13).

$$\alpha_{measurement} = 20(log(|Y1| + |Y2|) - log(|Y3| + |Y4|)). \quad (13)$$

Delay was obtained from the result of time difference between signal peaks with and without using a barrier and written on (14).

$$\Delta t_{measurement} = X3 - X1. \quad (14)$$

1) Measurement Results with the Hebel Brick Barrier: Detection of objects with a Hebel brick barrier was carried out at two distances, i.e., 75 cm and 125 cm, with a 10 cm-thick Hebel brick barrier. The distance between the barrier and the radar remained the same, which was 24 cm. From the obtained results, it could be seen that the signal received by the radar experienced a significant decrease in power, which could be seen from the peak-to-peak amplitude of the reflected signal. The amplitude value of the receive signal could be seen in the Y-axis coordinates. In addition, the delay of the reflected signal received by the radar could also be seen, the value of which was apparent from the X-axis coordinates.

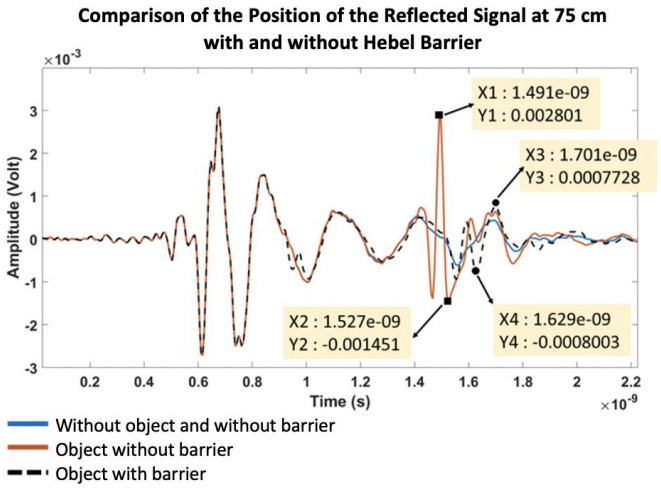

Fig. 6 Comparison of measurement results of reflected signal with and without the Hebel brick barrier at a distance of 75 cm.

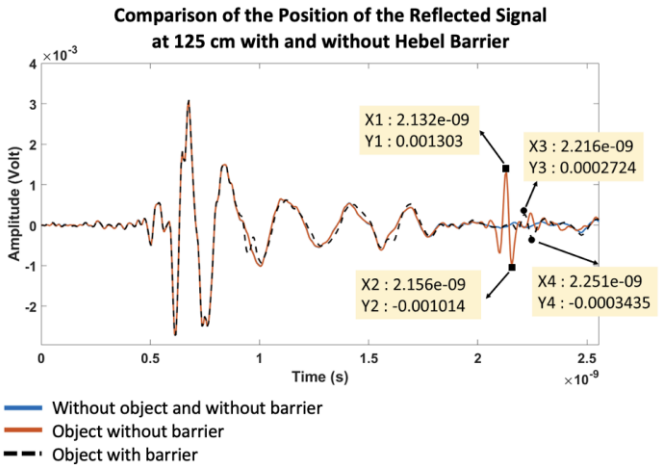

Fig. 7 Comparison of measurement results of reflected signals with and without the Hebel brick barrier at a distance of 125 cm.

Fig. 6 shows a comparison of the signals received by the radar with and without Hebel brick barriers at a distance of 75 cm. The amplitude of the received signal when using a Hebel brick barrier was lower than without a barrier. The decrease in power occurred at a distance of 75 cm was 8.636 dB. This decrease in power occurred because the wave experienced losses when propagating through the medium, so the power of the transmitted signal was smaller. These losses could be in the form of damping affected by the dielectric constant of the Hebel brick.

In addition, the Hebel brick barrier also caused a delay to the reflected signal received by the radar. The time difference of reflected signals received by the radar when utilizing the Hebel brick barrier and those were not can be seen in Fig. 6. The delay experienced by the waves propagating through the barrier was 0.21 ns. The presence of delay in object detection has caused

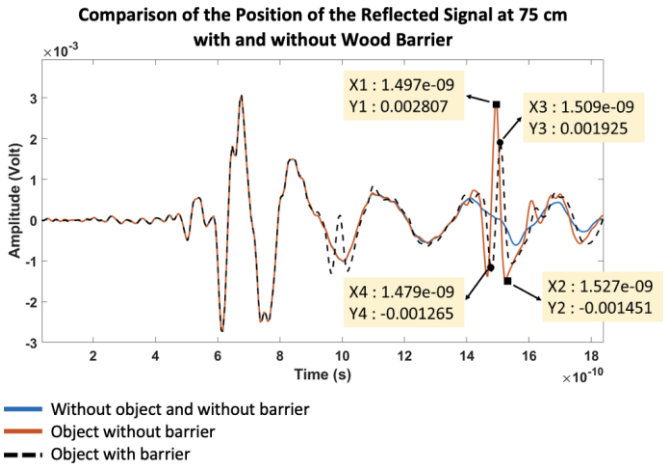

Fig. 8 Comparison of measurement results of reflected signals with and without wooden barriers at a distance of 75 cm.

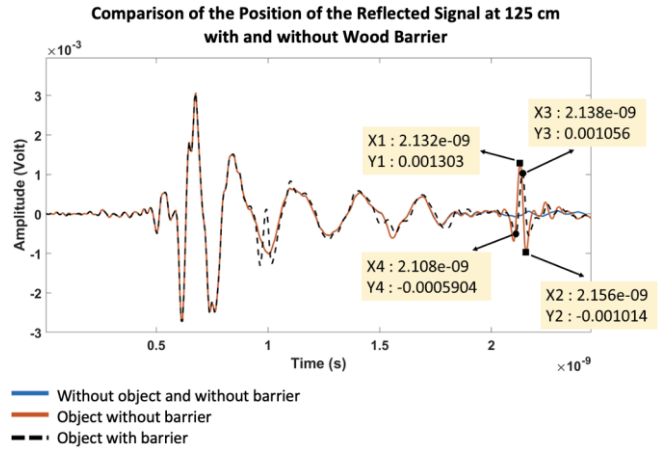

Fig. 9 Comparison of measurement results of reflected signals with and without wooden barriers at a distance of 125 cm.

the accuracy level of distance detection to decrease due to a shift in the position of the signal peak. The value of the shift of the signal's peak position in the detection using the Hebel brick barrier at a distance of 75 cm was 3.15 cm. At a distance of 125 cm, the occurring decrease in power, as shown in Fig. 7, was 11.51 dB, with a delay of 0.084 ns and the shift of the signal's peak position with barrier of 1.26 cm.

Fig. 6 and Fig. 7 show the effect of distance on detection results. The further the object is from the radar, the greater the decrease in reflected signal power received by the radar. It happens because the signal power at the time of reaching the object and returning to the radar is smaller due to the longer wave propagation distance. In addition, it can also be seen that the delay value of the reflected signal received by the radar is greater, corresponds with the distance of the object from the radar. It is due to farther wave propagation distance resulting in longer wave propagation times.

2) Measurement Results with Wooden Barriers: Detection of objects with wooden barriers was carried out with two distances, i.e., 75 cm and 125 cm, with a 2 cm-thick wooden barrier. The distance between the barrier and the radar remained the same, which was 24 cm. Delay was obtained from the time

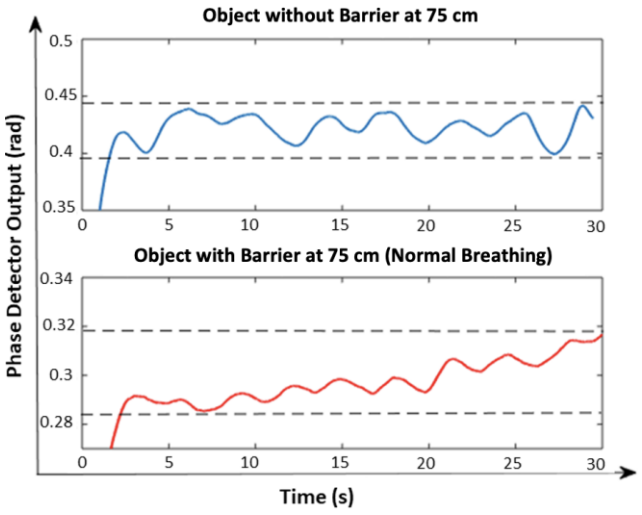

(a)

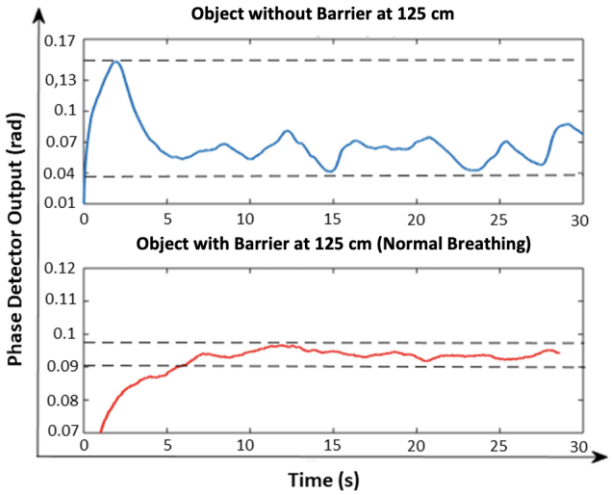

(b)

Fig. 10 Comparison of bladeRF detection results (a) objects at a distance of 75 cm (b) objects at a distance of 125 cm.

difference between signal peaks with and without using a barrier. The magnitude of delay value can be seen in the Y-axis coordinates. The results obtained are shown in Fig. 8 and Fig. 9. It is shown in the figure that the signal received by the radar experiences a decrease in power, which can be seen from the peak-to-peak amplitude of the reflected signal. The magnitude of the amplitude value can be seen from the coordinates of point X. The further the object is from the radar, the greater the decrease in reflected signal power received by the radar. It is the results of signal power being smaller when reaching the object and returning to the radar due to the longer wave propagation distance. In addition, it can also be seen that the delay of the reflected signal received by the radar, which causes a decrease in the accuracy level of distance detection due to the shift of the signal's peak position.

The decrease in power occurring at a distance of 75 cm was 2.51 dB with a delay of 0.12 ns and the shift of the signal's peak position with barrier of 0.18 cm. The decrease in power occurs because the wave experiences losses when propagating through

TABLE II
COMPARISON OF TOTAL ATTENUATION MEASUREMENT RESULTS USING CALCULATION AND VNA.

Barrier Type	Total Attenuation Calculation (dB)	Total Attenuation Using VNA (dB)	
		75 cm	125 cm
Hebel Brick	12.1	8.636	11.51
Wood	1.63	2.51	2.968

TABLE III
COMPARISON OF DELAY MEASUREMENT RESULTS USING CALCULATION AND VNA.

Barrier Type	Delay using Calculation (ns)	Delay Using VNA (ns)	
		75 cm	125 cm
Hebel Brick	0.563	0.21	0.084
Wood	0.094	0.12	0.006

the medium, so the power of the transmitted signal is smaller. These losses can be in the form of damping which is affected by the dielectric constant of the wood. The presence of delay in the object detection has led to the decrease in the accuracy level of distance detection due to the shift of the signal's peak position. The experimental results are shown in Fig. 8.

Meanwhile, at a distance of 125 cm, the decrease in power that occurred was 2.968 dB with a delay of 0.006 ns and the shift of the signal's peak with barrier of a 0.09 cm. The experimental results are shown in Fig. 9.

C. Measurement Results Using BladeRF

Measurement of the effect of the barrier on object detection using VNA was validated by measuring vital signs of breathing using a radar system modeled by bladeRF with several distances, i.e., 75 cm and 125 cm with wall barriers. Measurement data taken in the form of breathing samples for 30 s with a typical breathing model. The measurement results are shown in Fig. 10. The results obtained from the vital signs of breathing detection behind the walls indicate that the barrier wall affects the detection. Breathing pattern detection results when inhaling and exhaling without a barrier were clearer compared to those using a barrier. The upper peak on the wave indicates an air-inhaling event while the lower indicates an air-exhaling event. It has proven that the barrier wall exerts a significant effect on the detection of vital signs of breathing using a radar system.

D. Comparative Analysis of Measurement Results Using Calculations and VNA

In the measurement results using calculations, the dielectric constant greatly affected the losses resulting from each barrier. Based on the experiments that have been carried out, there are differences in the results obtained by measuring and calculating using VNA, as shown in Table II. Based on Table II, the measurement results of total attenuation using calculation are relatively close to the measurement results of total attenuation using VNA. However, the farther the object is from the antenna, the greater the difference in total attenuation. It occurs because measurements using calculations are not affected by distance. The size of the barrier in this experiment was also limited, so there was a diffraction effect from the edges of the wall, which then caused multipath waves from the radar to different targets. In addition, the further distance of the object from the radar caused the signal power reaching the object and returning to the radar to be smaller due to the more distant wave propagation.

According to Table III, the results of delay measurements using calculations and VNA indicate that the barrier causes a delay in the wave propagation. However, the results obtained in the measurement using calculation differs from those of using VNA. It happens because the results of measurements using VNA are not only influenced by the dielectric constant of the barrier, but also by other external factors, such as environmental conditions that can influence the wave propagation.

V. CONCLUSION

In this study, measurements on the vital signs of breathing detection without a barrier and using a radar system was performed. Measurement results using calculations and VNA indicate that the barrier provides significant losses. It is indicated by a decrease in the peak-to-peak amplitude of the signal at the time of measurement using the barrier. As a result of the smaller amplitude of the detected signal, the process of detecting the target is more difficult. The decrease in amplitude when using the Hebel brick barrier at the distance targets of 75 cm and 125 cm were 8.636 dB and 11.51 dB, respectively. On the other hand, the decrease in amplitude when using a wooden barrier at the distance targets of 75 cm and 125 cm were 2.51 dB and 2.968 dB, respectively. In addition, the thickness of the barrier has a significant effect on the total attenuation and delay at detection. The measurement results indicate that the barrier causes a delay to the reflected signal received by the radar. It is indicated by the shift of the peak position of the reflected signal when using the barrier, resulting in the reduced detection accuracy. The delays that occurred when using the Hebel brick barrier were 0.21 ns at a 75 cm-target distance cm and 0.084 ns at a 125 cm-target distance. At the same time, the delays that occurred when using a wooden barrier were 0.12 ns at a 75 cm-target distance and 0.006 ns at a 125 cm-target distance. Validation of experiments conducted using the bladeRF showed a barrier effect on vital signs of breathing detection. It is shown by the detection using barriers that causes the breathing pattern less visible, so there needs to be an effort to overcome this effect to obtain undisturbed detection accuracy. As a further study, it is possible to perform signal transmission by radar from different sides, other than the vertical side, to detect breathing in humans.

CONFLICT OF INTEREST

The author team declare that the article entitled "Effect of Barrier Walls on Detection of Breathing Vital Signs with Through-Wall Radar" is free from conflict of interest.

AUTHOR CONTRIBUTION

Conceptualization, methodology, Fildha Ridhia; validation, Aloysius Adya Pramudita, and Yuyu Wahyu; formal analysis,

Fildha Ridhia; writing—drafting of the original draft, Fildha Ridhia; writing—review and editing, Harfan Hian Ryanu; visualization, Fildha Ridhia, and Harfan Hian Ryanu; supervision, Aloysius Adya Pramudita and Yuyu Wahyu.

REFERENCES

[1] Z. Li, T. Jin, Y. Dai, and Y. Song, "Through-Wall Multi-Subject Localization and Vital Signs Monitoring Using UWB MIMO Imaging Radar," *Remote Sens*., Vol. 13, No. 15, pp. 1-21, Jul. 2021.

[2] T.O. Praktika, A.A. Pramudita, and Y. Wahyu, "Design of Vivaldi Antenna for UWB Respiration Radar," *2019 Int. Conf. Inf., Commun. Technol. (ICOIACT)*, 2019, pp. 11–16.

[3] S. Saleh, *et al*., "Compact UWB Vivaldi Tapered Slot Antenna," *Alexandria Eng. J*., Vol. 61, No. 6, pp. 4977–4994, Jun. 2022.

[4] A. Dell'Aversano, A. Natale, A. Buonanno, and R. Solimene, "Through the Wall Breathing Detection by Means of a Doppler Radar and MUSIC Algorithm," *IEEE Sensors Lett.*, Vol. 1, No. 3, pp. 1-4, Jun. 2017.

[5] K. Wang, Z. Zeng, and J. Sun, "Through-Wall Detection of the Moving Paths and Vital Signs of Human Beings," *IEEE Geosci., Remote Sens. Lett.*, Vol. 16, No. 5, pp. 717–721, May 2019.

[6] B.P.A. Rohman, M.B. Andra, and M. Nishimoto, "Through-the-Wall Human Respiration Detection Using UWB Impulse Radar on Hovering Drone," *IEEE J. Sel. Top. Appl. Earth Obs., Remote Sens.*, Vol. 14, pp. 6572–6584, Jun. 2021.

[7] F. Khan and S.H. Cho, "A Detailed Algorithm for Vital Sign Monitoring of a Stationary/Non-Stationary Human through IR-UWB Radar," *Sensors*, Vol. 17, No. 2, pp. 1-15, Feb. 2017.

[8] Z. Li, T. Jin, Y. Dai, and Y. Song, "Through-Wall Multi-Subject Localization and Vital Signs Monitoring Using UWB MIMO Imaging Radar," *Remote Sens.*, Vol. 13, No. 15, pp. 1-21, Jul. 2021.

[9] Z. Duan and J. Liang, "Non-Contact Detection of Vital Signs Using a UWB Radar Sensor*," IEEE Access*, Vol. 7, pp. 36888–36895, Apr. 2019.

[10] X. Liang, *et al*., "An Improved Algorithm for Through-Wall Target Detection Using Ultra-Wideband Impulse Radar," *IEEE Access*, Vol. 5, pp. 22101–22118, Oct. 2017.

[11] X. Zhang, *et al*., "Contactless Simultaneous Breathing and Heart Rate Detections in Physical Activity Using IR-UWB Radars," *Sensors*, Vol. 21, No. 16, pp. 1–18, Aug. 2021.

[12] H. Ryanu, D. Setiawan, and Edwar, "Desain Antena Mikrostrip UWB dengan Peningkatan Lebar Pita dan Karakteristik Triple Notch Band," *J. Nas. Tek. Elekt., Teknol. Inf.*, Vol. 10, No. 3, pp. 249–256, Aug. 2021.

[13] N.T. Kien and I.-P. Hong, "Evaluation of Common Building Wall in See-Through-Wall Application of Ultra-Wideband Synthetic Aperture Radar," *J. Elect. Eng., Technol.*, Vol. 16, pp. 437-442, Sep. 2020.

[14] R. Ambarini, A.A. Pramudita, E. Ali, and A.D. Setiawan, "Single-Tone Doppler Radar System for Human Respiratory Monitoring," *2018 5th Int. Conf. Elect. Eng. Comput. Sci., Inform. (EECSI)*, 2018, pp. 571–575.

[15] X. Li and G. Lv, "Improved Radiation Characteristics of Compact Antipodal Vivaldi Antenna with the Hybrid Technique for UWB Applications," *Electromagn.*, Vol. 41, No. 1, pp. 66–81, 2021.

[16] P.J. Gibson, "The Vivaldi Aerial," *Eur. Microw. Conf.*, 1979, pp. 101–105.

[17] J. Zhang, H. Lan, M. Liu, and Y. Yang, "A Handheld Nano Through-Wall Radar Locating with the Gain-Enhanced Vivaldi Antenna," *IEEE Sensors J.*, Vol. 20, No. 8, pp. 4420–4429, Apr. 2020.

[18] A.A. Pramudita, T.O. Praktika, and S. Jannah, "Radar Modeling Experiment Using Vector Network Analyzer," *2020 Int. Symp. Antennas, Propag. (ISAP)*, 2021, pp. 99–100.

[19] R. Akeela and B. Dezfouli, "Software-Defined Radios: Architecture, State-of-the-Art, Challenges," *Comput. Commun.*, Vol. 128, pp. 106–125, Sep. 2018.

[20] D. Garmatyuk, J. Schuerger, and K. Kauffman, "Multifunctional Software-Defined Radar Sensor and Data Communication System," *IEEE Sensors J.*, Vol. 11, No. 1, pp. 99–106, Jan. 2011.

[21] C. Apriono, F. Muin, and F.H. Juwono, "Portable Micro-Doppler Radar with Quadrature Radar Architecture for Non-Contact Human Breath Detection," *Sensors*, Vol. 21, No. 17, pp. 1–15, Aug. 2021.

[22] M. Gummineni and T.R. Polipalli, "Implementation of Reconfigurable Transceiver Using GNU Radio and HackRF One," *Wirel. Pers. Commun.*, Vol. 112, pp. 889–905, Jan. 2020.

[23] T.T.T. Quynh, *et al*., "Network Coding with Multimedia Transmission and Cognitive Networking: An Implementation Based on Software-Defined Radio," *REV J. Electron., Commun*., Vol. 10, No. 3–4, pp. 72–84, Jul.–Dec. 2021.